

# NJC

Accepted Manuscript



This is an *Accepted Manuscript*, which has been through the Royal Society of Chemistry peer review process and has been accepted for publication.

*Accepted Manuscripts* are published online shortly after acceptance, before technical editing, formatting and proof reading. Using this free service, authors can make their results available to the community, in citable form, before we publish the edited article. We will replace this *Accepted Manuscript* with the edited and formatted *Advance Article* as soon as it is available.

You can find more information about *Accepted Manuscripts* in the [Information for Authors](#).

Please note that technical editing may introduce minor changes to the text and/or graphics, which may alter content. The journal's standard [Terms & Conditions](#) and the [Ethical guidelines](#) still apply. In no event shall the Royal Society of Chemistry be held responsible for any errors or omissions in this *Accepted Manuscript* or any consequences arising from the use of any information it contains.



Journal Name

ARTICLE

## Synergistic effects of passivation treatment and nano-electrodeposition technologies on corrosion protection performance of electrogalvanized steel

Received 00th January 20xx,  
Accepted 00th January 20xx

DOI: 10.1039/x0xx00000x

[www.rsc.org/](http://www.rsc.org/)

Qingyang Li, Wang Ge, Jinqiu Zhang, Peixia Yang and Maozhong An\*

It is well known that surface nanocrystallization and passivation treatment are effective ways of improving corrosion resistance property of electrogalvanized steel, but their synergistic effects have rarely been studied. In this study, the effect of surface nanocrystallization on chromium-free passivation film of electrodeposited zinc coating is investigated. Meanwhile, the formation mechanism of chromium-free passivation film on electrodeposited zinc coating changing with the reduction of grain sizes from micro to nano-meters is analyzed and a model for the formation mechanism is proposed. The chromium-free passivation film of nanocrystalline zinc coating combines the advantages of passive films and nano-materials, has better corrosion protection performance than chromium-free passivation film of coarse-grained zinc coating and nanocrystalline zinc coating as well as mirror decorative effect with light blue color. The corrosion resistance property of coarse-grained zinc coating is heightened almost five times due to the synergistic effects of passivation treatment and nano-electrodeposition technologies.

### Introduction

Electrodeposited zinc coating has been extensively applied to enhance the corrosion resistance of steel by cathodic protection due to its low cost and easy application.<sup>1</sup> However, considering the sacrificial nature as well as poor corrosion resistance of zinc coating, passivation treatment is generally adopted for prolonging the lifetime of zinc coating, which protects the zinc coating against corrosion because it forms a non-reactive barrier to humid air and other corrosion environments. In addition to an effective corrosion protection, the passive films also provide different colors for zinc coating.<sup>2-7</sup> Nano-electrodeposition is another technology to improve the corrosion protection property of zinc coating, which as a versatile, convenient and flexible technique is receiving extensive attention in recent years. Nanocrystalline zinc electrodeposits have exhibited better mechanical, tribological and electrochemical performances than conventional coarse-grained counterpart due to their grain sizes below 100 nm and high-volume fraction of the grain boundary.<sup>8-10</sup> Different from the barrier effect of passive films to corrosion environments, the corrosion resistance improvement of a zinc coating with the reduction of grain size from micro to nano-scales is attributed to the fact that the nanocrystalline structure enhances the kinetics of passivation and the stability of

corrosion product layer formed on zinc coating during the exposure to corrosion mediums.<sup>11-15</sup> So far, many efforts have been made by researchers in order to investigate the corrosion behaviors of passive films and nanocrystalline zinc coatings in various corrosion media by different techniques.<sup>16-24</sup> However, the synergistic effects of passivation treatment and nano-electrodeposition technologies on the corrosion protection performance of electrogalvanized steel have been scarcely studied to date.

Based on the analyses above, we hope to improve the performances of electrogalvanized steel further by combining the advantages of nano-electrodeposition and chromium-free passivation technologies. For this reason, in this study, we synthesize the chromium-free passivation films on coarse-grained and nanocrystalline zinc coatings, respectively, and study the influence of grain size on the performances of chromium-free passivation film of zinc coatings from the morphology and corrosion protection performance points of view. In the meantime, a model of passive film formation mechanism on the surface of coarse-grained and nanocrystalline zinc coatings has been established, so as to explain the change of corrosion resistance of passive films with the reduction of grain sizes from micro to nano-scales.

### Experimental

#### Specimen preparation

The coarse-grained and nanocrystalline zinc coatings were produced on carbon steel by pulse reverse electrodeposition from a basic sulfate bath without or with the additive. The

<sup>a</sup> State Key Laboratory of Urban Water Resource and Environment, School of Chemical Engineering and Technology, Harbin Institute of Technology, Harbin 150001, China

† Electronic Supplementary Information (ESI) available. See DOI: 10.1039/x0xx00000x

thickness of coarse-grained and nanocrystalline zinc coatings is approximately 50 and 40  $\mu\text{m}$ , respectively (as shown in Fig. S1). After electrodeposition, the coatings were rinsed immediately in deionized water then submitted directly to chromium-free passivation treatment. Finally, the passive films were rinsed in deionized water and then dried using a dryer. The electrolyte and passivation solutions composition as well as experimental conditions is described in Table 1, and a detailed discussion of the experimental procedures is given elsewhere.<sup>25,26</sup> Both of coarse-grained and nanocrystalline zinc coatings as well as those passive films were produced under the same experimental conditions, and all experiments were duplicated while good reproducibility was obtained.

### Surface morphology and composition characterization

The surface morphologies, components and roughness of coarse-grained and nanocrystalline zinc coatings as well as those passive films were characterized by scanning electron microscope (FESEM, Helios Nanolab 600i) with energy dispersive X-ray spectroscopy (EDS) and surface profilometer (Form Talysurf PGI 1240, Taylor Hobson), respectively. Transmission electron microscopy (TEM, JEM-2100) was performed to determine the grain size of nanocrystalline zinc coating. Samples of nanocrystalline zinc coating were removed from the coating using a sapphire knife without destroying the substrate, and then dispersed in acetone. A drop of the solution was placed on a carbon-coated grid and inserted into the TEM. In addition, the color and brightness properties changing of the passive film with the reduction of grain size were explained by UV-vis spectrophotometer (PG, TU-1900). The spectrums were recorded in the range of visible light (between 380 and 750 nm) using  $\text{BaSO}_4$  as reference.

### Electrochemical corrosion behavior analysis

The corrosion protection performances of coarse-grained and nanocrystalline zinc coatings as well as those passive films were evaluated by potentiodynamic polarization technique at room temperature ( $25 \pm 1$  °C). Chloride-ion-induced corrosion

is a common situation for protective zinc coatings such as in marine environments,<sup>10</sup> hence the seawater is simulated using a 3.5 wt% NaCl solution and applied as the corrosive medium in this study. All electrochemical measurements were performed in a three-electrode cell using a CHI 750D electrochemical workstation with platinum plate, saturated calomel electrode (SCE) and zinc coatings (or passive films) with a geometrical working area of  $1 \times 1 \text{ cm}^2$  as the auxiliary, reference and working electrode, respectively. The working electrode was immersed in simulated seawater for 30 min before applying the current to establish a stable rest potential. Potentiodynamic polarization curves were obtained by changing the electrode potential in the range of  $\pm 500 \text{ mV}$  around the open-circuit potential (OCP) against SCE at a scan rate of  $1.0 \text{ mV s}^{-1}$ . After potentiodynamic polarization test, the surface morphology of zinc coatings and those passive films was observed using FESEM, and the corrosion areas of passive films were calculated by ImageJ2x software.

## Results and discussion

### Surface morphology and composition of passive films

Surface morphologies and elemental compositions of coarse-grained and nanocrystalline zinc coatings before and after chromium-free passivation treatment are shown in Fig. 1. It can be seen that coarse-grained zinc coating (Fig. 1a) preserves the hexagonal laminated structure of metal zinc and shows an irregular coarse-grained size. By comparing with coarse-grained zinc coating, nanocrystalline zinc coating (Fig. 1c) displays a uniform arrangement of crystals and refinement of crystal size. As clearly illustrated from TEM image (Fig. 2) of nanocrystalline zinc coating, the coating shows approximately spherical-shaped particles with average grain sizes around 40 nm. After passivation treatment, although both of the passive films on coarse-grained and nanocrystalline zinc coatings are mainly composed of Zn, O, Ti and P elements, and have not significantly changed in grain sizes (as shown in Figs. 1b and d), the chromium-free passivation treatment makes both zinc

**Table 1** Compositions and experimental conditions of electrodeposition as well as passivation bath.

Solution	Composition and experimental conditions			
Basic bath	$\text{Zn}_2\text{SO}_4 \cdot 7\text{H}_2\text{O}$	$100 \text{ g L}^{-1}$	Forward pulse current density	$3 \text{ A dm}^{-2}$
	$\text{H}_3\text{BO}_3$	$20 \text{ g L}^{-1}$	Reverse pulse current density	$0.3 \text{ A dm}^{-2}$
Additive	Polyacrylamide	$1 \text{ g L}^{-1}$	Forward pulse durations	100 ms
	pH	1-2	Reverse pulse durations	10 ms
	Temperature	25 °C	Duty cycle	20 %
	Magnetically stirred	Mild	Time	60 min
Passivation bath	$\text{TiCl}_3$	$10 \text{ ml L}^{-1}$	$\text{H}_2\text{SO}_4$	$1.8 \text{ ml L}^{-1}$
	$\text{H}_3\text{PO}_4$	$1.8 \text{ ml L}^{-1}$	$\text{HNO}_3$	$2.8 \text{ ml L}^{-1}$
	$\text{Na}_2\text{SiO}_3$	$18 \text{ g L}^{-1}$	Passivation times	25 s
	$\text{Na}_2\text{MoO}_4 \cdot 2\text{H}_2\text{O}$	$0.85 \text{ g L}^{-1}$	pH	1.5-2.5
	NaF	$0.4 \text{ g L}^{-1}$	Temperature	25 °C
	$\text{H}_2\text{O}_2$	$48 \text{ ml L}^{-1}$		

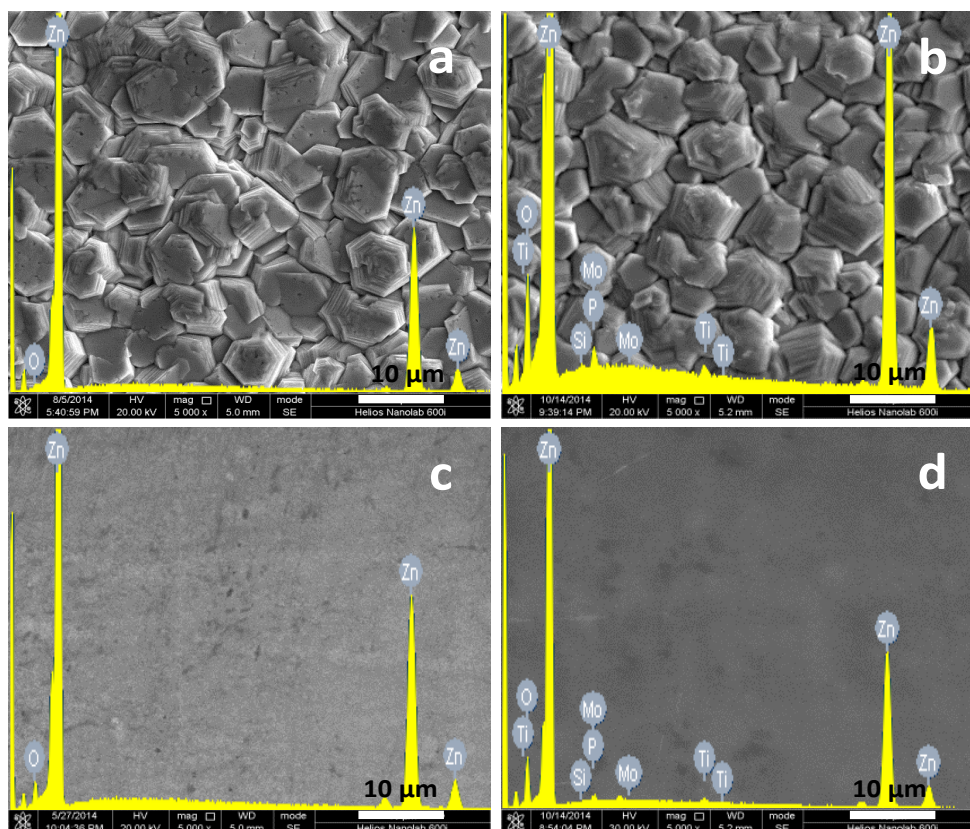


**Fig. 1** FESEM micrographs and EDS spectrums of coarse-grained (a) and nanocrystalline (c) zinc coatings, as well as their chromium-free passivation films (b, d). Images b and d correspond to the passive film of coarse-grained and nanocrystalline zinc coatings, respectively.

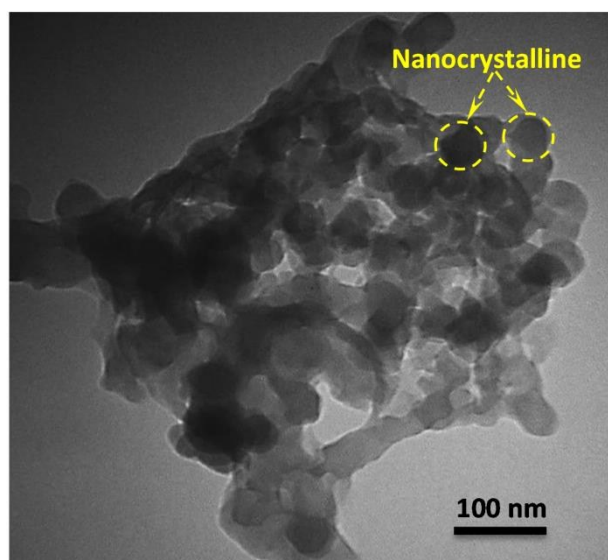


**Fig. 2** TEM image of nanocrystalline zinc scratched off from the coating.

coatings smoother (as shown in Fig. 3). Through the comparison of surface roughness profiles for coatings, passive films and substrate, the roughness of substrate is higher than that of nanocrystalline zinc coating (Fig. 3c) and its passive film (Fig. 3d), while lower than that of coarse-grained zinc

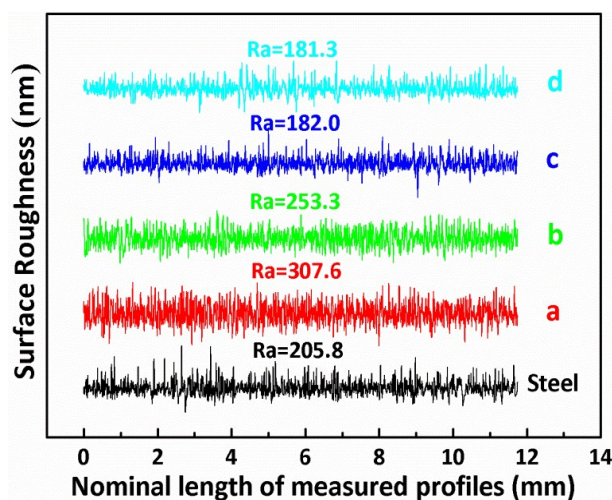


**Fig. 3** Surface roughness profiles and average roughness values (Ra) for steel substrate, coarse-grained (a) and nanocrystalline (c) zinc coatings, as well as the passive film of coarse-grained (b) and nanocrystalline (d) zinc coatings.

coating (Fig. 3a) and its passive film (Fig. 3b). It implies that the results of roughness measurement are not affected by substrate morphology and are reliable, as well as the surface nanocrystallization of zinc coating has significantly lowered the roughness of coarse-grained zinc coating and its passive film.

Moreover, it can also be seen from Fig. 4 that chromium-free passivation treatment also changes the color of coarse-grained and nanocrystalline zinc coatings from white (Figs. 4a and c) to light blue (Figs. 4b and d), indicating that the passivation treatment provides a certain decorative effect on both zinc coatings. Another notable difference is that nanocrystalline zinc coating (Fig. 4c) and its passive film (Fig. 4d) are mirror-bright and can reflect the icon clearly. However, the coarse-grained zinc coating and its passive film is dull and could not reflect any pattern. In order to investigate the reason of color and brightness difference between the passive films of coarse-grained and nanocrystalline zinc coatings, light reflectance properties of both zinc coatings and their passive films are measured by UV-vis reflectance spectra and as shown in Fig. 5. The basic line is made by BaSO<sub>4</sub>. It can be concluded from the difference between the spectrums of the passive films and the spectrums of the coatings that both of the reflectance of coarse-grained (Fig. 5a) and nanocrystalline (Fig. 5c) zinc coatings show obvious reduction after chromium-free passivation treatment (Fig. 5b and Fig. 5d correspond to the spectrum of the passive films on coarse-grained zinc coating

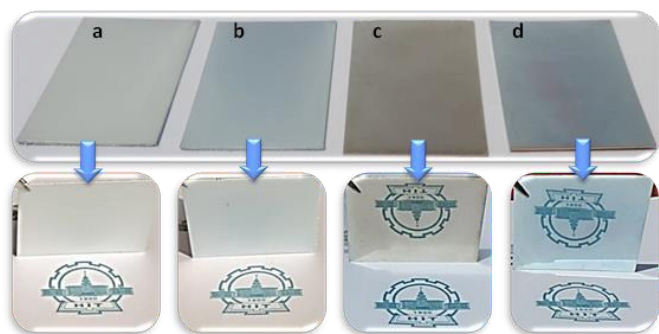


Fig. 4 Photographs of coarse-grained zinc coating (a) and its passive film (b), as well as nanocrystalline zinc coating (c) and its passive film (d).

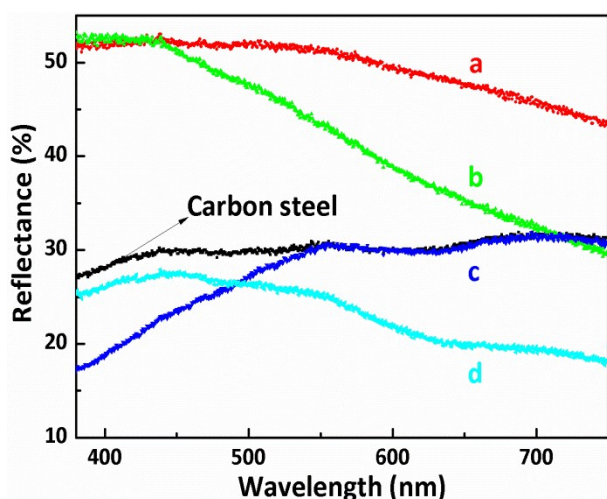


Fig. 5 UV-vis reflectance spectra of carbon steel, coarse-grained zinc coating (a) and its passive film (b), as well as nanocrystalline zinc coating (c) and its passive film (d) with BaSO<sub>4</sub> as basic line.

and nanocrystalline zinc coating, respectively). Another noteworthy part of the spectrums is the reflectance of the coarse-grained zinc coating and its passive film is higher than that of the nanocrystalline zinc coating and its passive film, which can be ascribed to the surface nanocrystallization of zinc coating. The difference of reflectance is the reason why the coarse-grained and nanocrystalline zinc coatings as well as these passive films show different colors and brightnesses.

#### Corrosion protection performances of passive films

The corrosion resistance properties of coarse-grained and nanocrystalline zinc coatings as well as their passive films in 3.5 wt% NaCl solution are evaluated through potentiodynamic polarization technique, and these polarization curves are shown in Fig. 6. A summary of the corrosion potentials ( $E_{corr}$ ), anodic and cathodic Tafel slopes ( $\beta_a$  and  $\beta_c$ ), as well as corrosion currents ( $i_{corr}$ ) derived from the polarization curves is also listed in Table 2. The  $E_{corr}$ ,  $\beta_a$  and  $\beta_c$  were calculated from the polarization curves using linear extrapolation method. Then, the  $i_{corr}$  of conversion films was calculated by means of the Stern-Geary equation as follows (1).<sup>27</sup>

$$i_{corr} = \frac{\beta_a \times \beta_c}{2.303 \times R_p(\beta_a + \beta_c)} \quad (1)$$

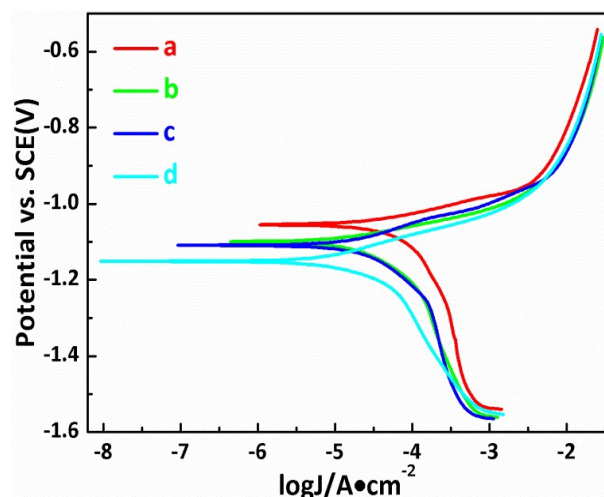


Fig. 6 Polarization curves of coarse-grained zinc coating (a) and its passive film (b), as well as nanocrystalline zinc coating (c) and its passive film (d) in 3.5 wt% NaCl solution at 25 ± 1°C.

Table 2 Electrochemical parameters of coarse-grained zinc coating (a) and its passive film (b), as well as nanocrystalline zinc coating (c) and its passive film (d) in 3.5 wt% NaCl solution at 25 ± 1°C.

Sample	$E_{corr}$ mV	$\beta_a$ mV dec <sup>-1</sup>	$\beta_c$ mV dec <sup>-1</sup>	$R_p$ $\Omega$ cm <sup>2</sup>	$i_{corr}$ $\mu$ A cm <sup>-2</sup>
a	-1055	60.2	289.2	450.4	48.1
b	-1100	64.1	168.2	1031.0	19.5
c	-1109	51.1	173.5	918.7	18.6
d	-1151	51.9	215.9	1744.0	10.4

Where  $R_p$  is the linear polarization resistance determined by the slope of current-potential plot in the range of  $\pm 2$  mV around the corrosion potential according to equation (2).<sup>28</sup>

$$R_p = \left( \frac{dE}{di} \right)_{i \rightarrow 0} \quad (2)$$

It can be seen that both chromium-free passivation treatment ( $i_{corr}^b = 19.5 \mu\text{A cm}^{-2}$ ) and surface nanocrystallization ( $i_{corr}^c = 18.6 \mu\text{A cm}^{-2}$ ) significantly improve the corrosion resistance property of coarse-grained zinc coating ( $i_{corr}^a = 48.1 \mu\text{A cm}^{-2}$ ). And the chromium-free passivation film of nanocrystalline zinc coating ( $i_{corr}^d = 10.4 \mu\text{A cm}^{-2}$ ) combines the advantages of passive films and nanomaterials, therefore has a better corrosion protection performance than nanocrystalline zinc coating and passive film of coarse-grained zinc coating. The corrosion resistance property of coarse-grained zinc coating is heightened almost five times due to the synergistic effects of passivation treatment and nano-electrodeposition technologies.

After potentiodynamic polarization test, FESEM observation is carried out for coarse-grained and nanocrystalline zinc coatings as well as their passive films, as shown in Fig. 7. Significant differences can be observed in the corroded surfaces of both zinc coatings before and after chromium-free passivation treatment. There are many cracks on the surface

of coarse-grained zinc coating, indicating that the corrosion sites are local and corroded badly (Fig. 7a). As for nanocrystalline zinc coating, some small and shallow etch-pits are discretely distributed over the corroded surface (Fig. 7c), which indicates a better protection surface film. In comparison between the corroded surfaces of the coatings and their passive films, both coatings show less corrosion sites after passivation treatment (as shown in Figs. 7b and d), which is due to the fact that the insoluble passive films on the surface of coarse-grained and nanocrystalline zinc coatings inhibit corrosion further, and the corrosion is initiated by defect sites of the film. However, it is noteworthy that although both passive films have a protective effect for coarse-grained and nanocrystalline zinc coatings during the electrochemical corrosion in NaCl solution, the passive film of nanocrystalline zinc coating (Fig. 7d) shows lower defect rates ( $\eta$ ) than the passive film of coarse-grained zinc coating (Fig. 7b) under the same corrosion conditions. The  $\eta$  of passive films on the surface of coarse-grained and nanocrystalline zinc coatings calculated by ImageJ2x software are approximately 70.51% and 46.15%, respectively (The detailed calculation process is illustrated in Fig. S2.). All of the above analytical results indicate that the synergistic effects of passivation treatment and nano-electrodeposition technologies effectively improve the corrosion protection performance of electrogalvanized steel further.

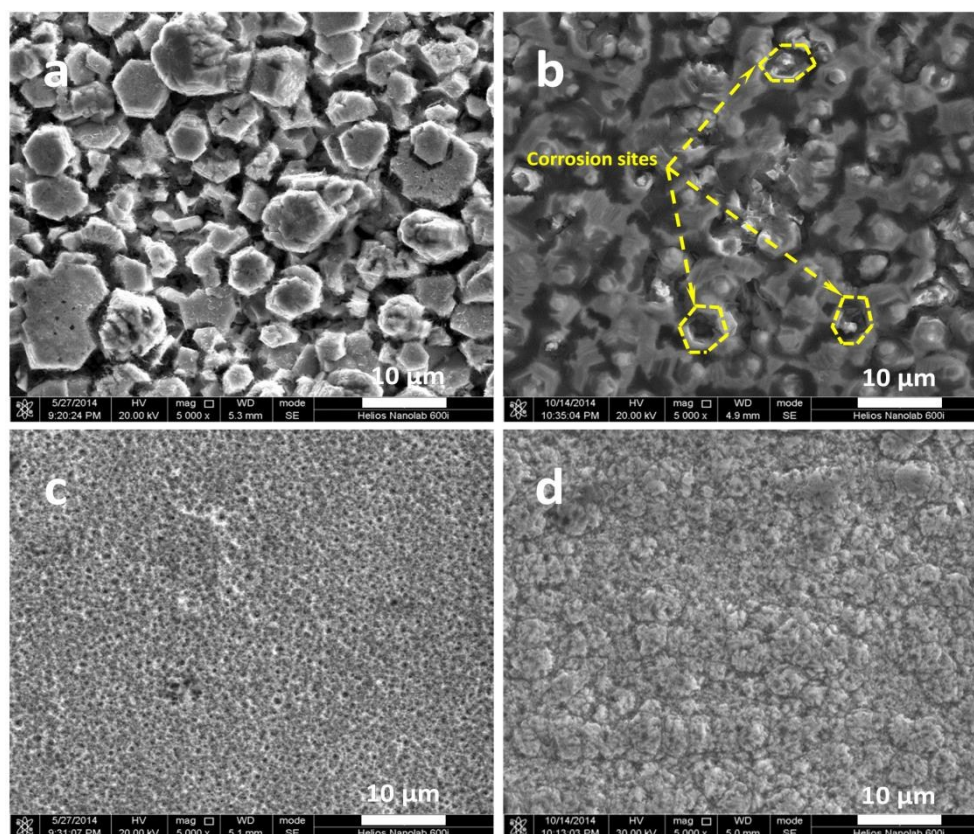


**Fig. 7** Surface morphologies of coarse-grained zinc coating (a) and its passive film (b), as well as nanocrystalline zinc coating (c) and its passive film (d) after potentiodynamic polarization test.

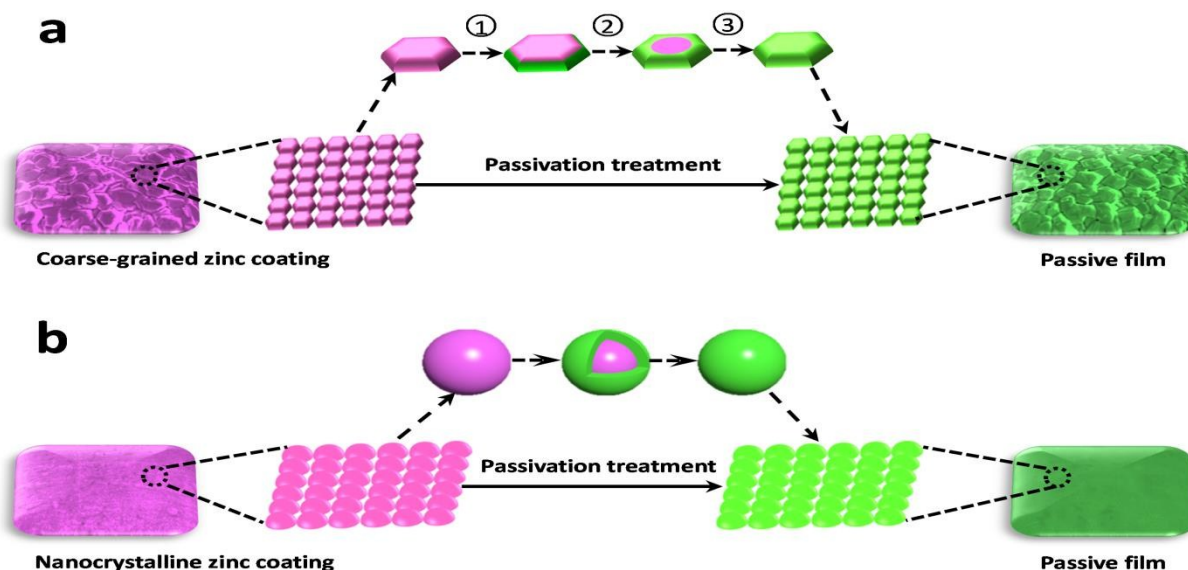


**Fig. 8** Model for the formation mechanism of passive films on the surface of coarse-grained (a) and nanocrystalline (b) zinc coatings during chromium-free passivation treatment.

The corrosion resistance improvement of the passive film on zinc coatings with the reduction of grain size from micro to nano-scale can be explained by the formation mechanism changing of passive films. According to previous research,<sup>15</sup> the passivation behavior of coarse-grained zinc coating first takes place in the thickness direction (as shown in step ① of Fig. 8a) of the crystalline grains and gradually extends to the most part of the crystalline surface (Fig. 8a ②), thereby forms a layer of complete passive layer on the coarse-grained zinc (Fig. 8a ③). Therefore, the passive film of coarse-grained zinc coating is nonuniform as well as defective (as shown in Fig. S3.). This growth mode of passive film on coarse-grained zinc coating is due to the fact that the zinc atoms at the grain boundaries possess a higher activity and the coating only achieves nanoscale in the thickness direction of zinc crystalline grains (as shown in Fig. S4.), therefore the passivation behavior preferentially takes place in the thickness direction of coarse-grained zinc during exposure to passivation bath. As for nanocrystalline zinc coating, it achieves the nanoscale in three-dimensional space, so zinc atoms that are exposed on the surface of the coating possess a higher activity. This is beneficial for diffusion of passivation reaction during exposure to chromium-free passivation bath, thus promoting the formation of a denser, more uniform and stable passive film and contributing to corrosion protection property enhancement. Therefore, the passive film on the surface of nanocrystalline zinc coating (as shown in Fig. S5) has fewer defects than the passive film of coarse-grained zinc coating (in Fig. S3). In this case, the corrosion resistance differences between the passive film of coarse-grained and nanocrystalline zinc coatings are ascribed to the fact that nano-structure of nanocrystalline zinc coating enhances kinetics of passivation and stability of the formed passive film.

## Conclusions

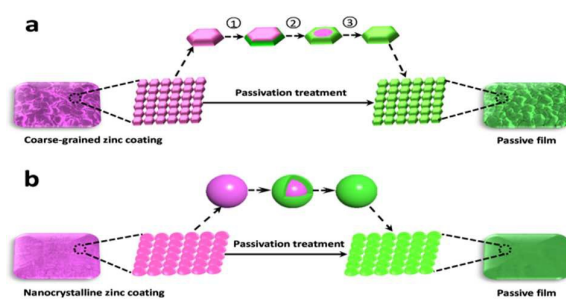
This paper mainly describe the influence of surface nanocrystallization on corrosion behaviors of chromium-free passivation film on conventional coarse-grained zinc coating, which is to give insight into the synergistic effects of passivation treatment and nano-electrodeposition technologies on corrosion protection performance of electrogalvanized steel. The chromium-free passivation film of nanocrystalline zinc coating combines the advantages of passive films and nano-materials, exhibits a uniform, dense and smooth surface morphology as well as light blue mirror-bright performance. Specially, the corrosion protection performance of chromium-free passivation film on nanocrystalline zinc coating is better than that of chromium-free passivation film on coarse-grained zinc coating as well as nanocrystalline zinc coating, which is almost five times that of the coarse-grained zinc coating. The performance improvement of chromium-free passive film on conventional coarse-grained zinc coating with the reduction of grain sizes from micro to nano-meters is attributed to the fact that the fine grain size and the high grain boundary volume fraction of nanocrystalline zinc coating enhances kinetics of passivation reaction as well as stability of the formed passive film. The formation mechanism model of the chromium-free passivation film on zinc coating is put forward corresponding to the grain size reduction.

## References

- 1 C. Y. Tsai, J. S. Liu, P. L. Chen and C. S. Lin, *Corros. Sci.*, 2010, **52**, 3385.
- 2 H. Y. Su and C. S. Lin, *Corros. Sci.*, 2014, **83**, 137.
- 3 G. Kong, J. T. Lu, S. H. Zhang, C. S. Che and H. J. Wu, *Surf. Coat. Technol.*, 2010, **205**, 545.
- 4 C. R. Tomachuk, C. I. Elsner, A. R. Di Sarli and O. B. Ferraz, *Mater. Chem. Phys.*, 2010, **119**, 19.
- 5 Y. T. Chang, N. T. Wen, W. K. Chen, M. D. Ger, G. T. Pan and T. C. K. Yang, *Corros. Sci.*, 2008, **50**, 3494.

- 6 Y. T. Tsai, K. H. Hou, C. Y. Bai, J. L. Lee and M. D. Ger, *Thin Solid Films*, 2010, **518**, 7541.
- 7 M. Hara, R. Ichino, M. Okido and N. Wada, *Surf. Coat. Technol.*, 2003, **169**, 679.
- 8 K. Saber, C. C. Koch and P. S. Fedkiw, *Mater. Sci. Eng., A*, 2003, **341**, 174.
- 9 Q. Y. Li, Z. B. Feng, L. H. Liu, J. Sun, Y. T. Qu, F. H. Li and M. Z. An, *RSC Adv.*, 2015, **5**, 12025.
- 10 M. C. Li, L. L. Jiang, W. Q. Zhang, Y. H. Qian, S. Z. Luo and J. N. Shen, *J. Solid State Electrochem.*, 2007, **11**, 1319.
- 11 K. M. Youssef, C. C. Koch and P. S. Fedkiw, *Corros. Sci.*, 2004, **46**, 51.
- 12 R. Ramanauskas, L. Gudavičiūtė, R. Juškėnas and O. Ščit, *Electrochim. Acta*, 2007, **53**, 1801.
- 13 L. P. Wang, Y. M. Lin, Z. X. Zeng, W. M. Liu, Q. J. Xue, L. T. Hu and J. Y. Zhang, *Electrochim. Acta*, 2007, **52**, 4342.
- 14 L. Liu, Y. Li, F. H. Wang, *Electrochim. Acta*, 2008, **53**, 2453.
- 15 Q. Y. Li, Z. B. Feng, L. H. Liu, H. Xu, W. Ge, F. H. Li and M. Z. An, *RSC Adv.*, 2015, **5**, 32479.
- 16 N. T. Wen, C. S. Lin, C. Y. Bai and M. D. Ger, *Surf. Coat. Technol.*, 2008, **203**, 317.
- 17 B. L. Lin, J. T. Lu and G. Kong, *Surf. Coat. Technol.*, 2008, **202**, 1831.
- 18 R. P. Socha, N. Pommier and J. Fransaer, *Surf. Coat. Technol.*, 2007, **201**, 5960.
- 19 K. Aramaki, *Corros. Sci.*, 2007, **49**, 1963.
- 20 R. Berger, U. Bexell, T. M. Grehk and S. E. Hörnström, *Surf. Coat. Technol.*, 2007, **202**, 391.
- 21 M. S. Chandrasekar and P. Malathy, *Mater. Chem. Phys.*, 2010, **124**, 516.
- 22 G. Meng, L. Zhang, Y. Shao, T. Zhang and F. Wang, *Corros. Sci.*, 2009, **51**, 1685.
- 23 H. B. Muralidhara and Y. A. Naik, *Bull. Mater. Sci.*, 2008, **31**, 585.
- 24 H. B. Muralidhara, J. Balasubramanyam, Y. A. Naik, K. Y. Kumar, H. Hanumanthappa and M. S. Veena, *J. Chem. Pharm. Res*, 2011, **3**, 433.
- 25 Q. Y. Li, Z. B. Feng, J. Q. Zhang, P. X. Yang, F. H. Li and M. Z. An, *RSC Adv.*, 2014, **4**, 52562.
- 26 J. Q. Zhang, M. Z. An, C. X. Li and P. X. Yang, *Electroplat. Pollut. Control.*, 2013, **5**, 33 (Chinese with English abstract).
- 27 M. Stern and A. L. Geary, *J. Electrochem. Soc.*, 1957, **104**, 56.
- 28 M. Mouanga, L. Ricq, G. Douglade, J. Douglade and P. Berçot, *Surf. Coat. Technol.*, 2006, **201**, 762.





A theoretical model of passive film formation mechanism on coarse-grained (a) and nanocrystalline (b) zinc coatings is proposed.